Optics and Laser Technology 103 (2018) 233–238

Contents lists available at ScienceDirect

Optics and Laser Technology

journal homepage: www.elsevier.com/locate/optlastec

Full length article

Optical properties and antimicrobial effects of silver nanoparticles synthesized by femtosecond laser photoreduction

Daniella dos Santos Courrol [a], Carla Regina Borges Lopes [b], Thiago da Silva Cordeiro [c], Marcia Regina Franzolin [a], Nilson Dias Vieira Junior [c], Ricardo Elgul Samad [c], Lilia Coronato Courrol [b,*]

[a] Laboratório de Bacteriologia, Instituto Butantan, São Paulo, SP, Brazil
[b] Laboratório de Lasers e Óptica Biomédica Aplicada, Universidade Federal de São Paulo, Departamento de Física, Diadema, SP, Brazil
[c] Centro de Lasers e Aplicações, IPEN-CNEN/SP, São Paulo, SP, Brazil

ARTICLE INFO

Article history:
Received 11 December 2017
Received in revised form 13 January 2018
Accepted 15 January 2018

Keywords:
Silver nanoparticles
Microorganisms
Laser
Femtosecond
Tryptophan

ABSTRACT

Silver nanoparticles exhibit a powerful antimicrobial action showing a pronounced potential to be widely used against drug resistance bacteria. The present work describes the optical properties and antimicrobial effect of silver nanoparticles produced by femtosecond laser photoreduction of $AgNO_3$ in the presence of tryptophan water solution. The advantages of this method are the absence of hazardous chemical reducing agents in the solution, and the versatile dimensional control achieved. The synthesized silver nanoparticles were characterized by absorption and fluorescence spectroscopy and their antibacterial activity were determined by monitoring the cell viability of *Escherichia coli*. The effects of the silver nanoparticles concentration and laser parameters (exposure time and pulse energy), on the formation of the nanoparticles, and its influence on the bacteria growth inhibition were studied. The prepared silver nanoparticles exhibited suitable antimicrobial properties. The results demonstrated that the nanoparticles concentration plays an important role in their bactericidal efficacy. The increase in the laser energy caused an increase in *E. coli* growth inhibition. Irradiations with energies around 300 μJ for 60 min presented high antimicrobial activity due to the presence of kynurenine, sub product of tryptophan photolysis. The first-time formation mechanism of tryptophan silver nanoparticles in high optical intensities was also discussed.

1. Introduction

Silver nanoparticles are an effective tool for killing microorganisms and have been used in catheters, bandages, water purification, cosmetics, toys, clothing, etc [1–3]. These nanoparticles have a broad spectrum of antibacterial properties against a wide range of gram-positive and gram-negative bacteria and do not contribute in the development of resistant strains [4], showing a great potential to be widely used against drug resistance bacteria.

Silver nanoparticles can be synthesized by a large variety of chemical, physical and biological methods [1,5,6], and among them, photoreduction by femtosecond laser pulses is used to produce nanoparticles with controlled sizes and concentrations [7,8]. The advantages of this method are the absence of hazardous chemical reducing agents in the solution, and the versatile dimensional control achieved. When synthesizing nanoparticle with focalized laser pulses, the temporal scale is the main parameter for the metallic nanoparticle fragmentation. On the femtosecond scale, the most common fragmentation process is the Coulomb explosion [9]. Several parameters such as the laser wavelength, intensity, pulse energy, pulse duration, repetition rate, influence in the growth and the aggregation mechanisms, and their control define the final size of the nanoparticles.

When silver nanoparticles interact with bacteria they produce reactive oxygen species and impairment of flagellar activity, which were observed for a broad range of silver species [10], and are responsible for bacteria inhibition [11]. Silver nanoparticles induce DNA degradation [11]. Inside the bacteria, spherical NPs interact and destroy the sulfur and phosphorus-containing complexes (soft bases) like DNA, and also disrupt the morphology of the membrane, finally leading to the cell death [12]. For a given quantity of silver, smaller nanoparticles show better inhibitory action due to a significantly larger surface area in contact with the bacterial effluent, resulting from the higher surface to volume ratio as compared to bigger nanoparticles. Therefore, smaller particles release more silver ions than larger particles to kill bacteria. Recently Raza et al. [12] observed that spherical silver nanoparticles with

* Corresponding author.
E-mail address: lccourrol@gmail.com (L. Coronato Courrol).

https://doi.org/10.1016/j.optlastec.2018.01.044
0030-3992/

diameters in the range 15–50 nm exhibited maximum bactericidal efficacy against *E. coli* strains, followed by the antibacterial activity of triangular silver nanoparticles. Dror-Ehre et al. [13] showed that the bactericidal activity of silver nanoparticles against *E. coli* relies on the ratio NPs/cells, which determines the frequency of collisions of the NPs to the cells. Furthermore, the antibacterial performance of these particles was observed to be even better than that of Ciprofloxacin, suggesting that silver nanoparticles can be a good alternative for antibiotics that have promoted bacterial resistance.

The use of amino acid tryptophan (Trp) in nanoparticle synthesis as reducing/stabilizing agent has been reported in the literature [14–18]. The main advantages of using tryptophan in the synthesis of silver nanoparticles are low toxicity, biocompatibility, and ability to load various bioactive molecules potentializing drug delivery. Tryptophan nanoparticles can reduce potential hepato and nephrotoxicity [16]. Mukha et al. observed that the formation and stabilization of gold and silver nanoparticles in the presence of tryptophan is strongly influenced by acidity of initial components, and the tryptophan conversion in such systems goes through the kynurenine pathway [17].

The present study reports the synthesis of tryptophan silver nanoparticles by femtosecond laser pulses, investigating the effects of concentration and laser parameters (exposure time and pulse energy) on the formation of the nanoparticles and its influence on the bacteria growth inhibition. The formation mechanism of tryptophan silver nanoparticles in high optical intensities is also discussed.

2. Materials and methods

The green and environment friendly method to synthesize silver nanoparticles with ultrashort laser pulses for antimicrobial applications is described in the following paragraphs.

2.1. First Experiment: Concentration dependence

All the reagents used had analytical grade. Silver nitrate and commercial L-Tryptophan Vetec were purchased from Sigma–Aldrich. Initially, tryptophan silver nanoparticles (TrpAgNPs) solutions with different silver concentrations were prepared mixing $AgNO_3$ with tryptophan, according to Table 1, in 100 mL of distilled water at room temperature. The process was accompanied by vigorous stirring for 5 min.

The solutions 2, 3 and 4 were irradiated by 40 fs ultrashort pulses from an amplified Ti:Sapphire laser system (Odin, from Quantronix), centered at 800 nm, 400 μJ of maximum energy, at 1 kHz repetition rate. The laser beam was focused by a 50 mm lens, inside a 1 cm glass cuvette containing 1 mL of solutions, in such a way that no damage, or supercontinuum generation, occurred in the cuvette walls. Each solution was irradiated by 5 min in the first experiment.

2.2. Second Experiment: Irradiation time duration dependence

Solution 3 (1 mL) was irradiated with femtosecond pulses of 300 μJ, 40 fs pulses, 1 kHz, by 10, 20, 40 and 60 min.

2.3. Third Experiment: Pulse energy dependence

The influence of the pulses energy was studied (solution 3), fixing the irradiation time in 5 min, 1 kHz repetition rate and energies of 100, 200, 300, 350 and 400 μJ.

Table 1
Reagents used in TrpAgNps synthesis.

Sample	$AgNO_3$	Tryptophan
1	–	0.0621 g
2	0.0081 g	0.0621 g
3	0.0137 g	0.0617 g
4	0.0239 g	0.0618 g

2.3.1. Sample characterization

The UV–Vis absorption spectra of all samples were measured by a MultiSpec-1500 spectrophotometer (Shimadzu Scientific Instruments), using 1 cm quartz cells.

Fluorescence measurements were performed using a RF-5301 fluorimeter (Shimadzu Scientific Instruments). The samples fluorescence spectra under excitation at 280 nm were measured between 300 and 550 nm. All measurements were carried out at room temperature using a quartz cuvette with four polished faces and 1 mm of optical path.

Microscopic analyses were performed on a LEO 906E transmission electron microscope (Zeiss, Germany), with images captured using a Megaview III camera (Zeiss) and processed using the iTEM – Universal software HAS Imaging Platform (Olympus Soft Imaging Solutions GmbH, Germany). For analysis, 5 μl of each sample were deposited on a square copper mesh (37 μm/side), previously coated with parlodium and an amorphous carbon film. After allowing the sample to soak into the mesh (3 min), the excess sample was removed using absorbent paper and subjected to analysis. The ImageJ 1.46 software program was used to determine the average size of the nanoparticles by applying the Gaussian fitting in Origin 8.

Fourier Transforms Infra-Red spectroscopy (FTIR) of dried TrpAgNPs were grinded with KBr to make pellet and spectra was recorded using Shimadzu Spectrophotometer IRPrestige-21 in the region of 4000–700 cm^{-1}.

2.3.2. Growth inhibition assay

The *E. coli* ATCC 25,922 was transferred from glycerol (30 μl) to the culture medium TSB (trypticase soy broth), and left overnight in an incubator at 37 °C with 20% of CO_2. On the second day, the inoculum was transferred to the culture medium TSA (trypticase soy agar), and again incubated overnight at 37 °C with 20% of CO_2. On the third day, a solution of this inoculum was prepared at 0.5 McFarland scale, corresponding to 10^8 CFU/ml. This solution was prepared with saline 0.85% and a purview of the colony in TSA. After two dilutions in Mueller Hinton broth (MH) sterile, the solution final concentration was 10^6 CFU/ml.

The TrpAgNPs solutions obtained from the three experiments were diluted ten times in broth Mueller Hinton (20 μL of TrpAgNps + 180 μL MH). The viability tests were done in flat-bottom microplates (96 wells), in duplicate. 50 μl of TrpAgNps and 50 μL of inoculum were placed in each well. A control of TrpAgNps, was also made in duplicate, using 50 μL of TrpAgNps and 50 μl MH. Two wells were used for bacteria positive control (bacteria without nanoparticles), with 50 μL of inoculum and 50 μL MH. The plates were further incubated for 24 h at 37 °C. For cell viability study, after treatments for the microplate was placed in an incubator at 37 °C with 20% CO_2, and the reading was done by an ELISA reader at 595 nm. The percentage cell inhibition was calculated by the following formula:

$$\%\ \text{Cell inhibition} = 100 \times (\text{O.D. of control} - (\text{O.D. of treated} - \text{O.D. TrAgNPs}))/\text{O.D. of control}$$

were O.D is the Optical Density

Statistical analysis was done by Student's t-test. $P < .05$ was considered as significant.

3. Results

Fig. 1a shows the absorption spectra of solutions obtained from different $AgNO_3$ starting concentrations irradiated by ultrashort pulses (first experiment), compared to a non-irradiated sample (0.0137 g and $AgNO_3$ and 0.0617 g Trp). These spectra evidence a Surface Plasmon Resonance (SPR) [14] peaks around 422 nm in solutions 2 and 3 and sizes ~16 nm as shown the TEM image (insert figure). The absorption spectrum of solution 4 shows the SPR peak clearly broadened, indicating a second plasmon resonance shifted to longer wavelengths. This shift to ~520 nm indicates the presence of bigger particles (~80 nm). This formation of bigger particles is probably due to the higher concentration of silver nitrate in sample 4, which facilitates the aggregation of fragments resulting from the laser induced Coulomb explosion [19].

Fig. 1b presents the TrpAgNPs fluorescence around 350 nm, due to the tryptophan, when excited at 280 nm. A decrease in the emission band, without any shift of the emission maxima, can be observed with the increase in the silver nanoparticles concentration. The shape and full-width at half maximum (FWHM) of the absorption and emission bands also remain unchanged. The changes in the tryptophan emission band, are attributed to changes in the tryptophan environment due to the presence of silver nanoparticles, indicating that the silver nanoparticles can effectively quench the intrinsic fluorescence of tryptophan [20,21].

Fig. 2 presents the results obtained for sample 3 non-irradiated and irradiated by ultrashort pulses for different time durations, 10, 20, 40 and 60 min – (second experiment). Fig. 2a shows the absorption spectra of the solutions, revealing an increase in the TrpAgNps SPR intensity band with growing irradiation time up to 40 min. As the irradiation time increased up to 40 min, the solution SPR peak narrowed, indicating more homogeneous solutions. As the irradiation time increase to 60 min, the solution showed a decrease of the SPR band intensity.

Fig. 2b shows tryptophan fluorescence spectra obtaining exciting samples at 280 nm. In this figure it is observed a drastic tryptophan emission that follow absorption bands reduction for samples irradiated by 40 and 60 min.

Fig. 3 shows the photos and absorption spectra of the TrpAgNPs solutions obtained with pulse energies from 100 to 400 μJ (40 fs, 800 nm, 1 kHz, 5 min). The higher the laser energy, higher nanoparticles concentration in solution.

The FTIR spectra of tryptophan water solution and solution 3 irradiated by laser (300 μJ, 5 min) are shown in the Fig. 4. Is possible to observe bands relating to vibrations of carboxyl (1665 and 1417 cm^{-1}) and α-amine (3065, 1592, 1457 and 1009 cm^{-1}) and bands assigned to pyrrole (3410, 1355, 1098, 1009 and 861 cm^{-1}) and benzene (3033, 1355, 1231, 985, 861 and 743 cm^{-1}) rings from the indole side group [22]. The results obtained for TrpAgNPs indicated a decrease in the intensity followed by the increase in broadness of the peaks in the range between 1800 and 800 cm^{-1}, when compared with pure tryptophan, and the appearance of a peak at 1383 cm^{-1} to stretching and deformation vibrations of the carboxyl group.

The growth inhibition of *E. coli* in the presence of different TrpAgNPs synthesized with different $AgNO_3$ concentration is shown in Fig. 5a. The data comes from the experiments performed in duplicate referring to the incubation periods of 24 h. The results indicate that the silver nanoparticles strongly inhibit the growth of *E.coli*. After 24 h of incubation the inhibition of samples 3 and 4 are close to 100%, while for the sample 2 the inhibition efficiency is ~65%.

Fig. 5b shows *E. coli* growth inhibition with irradiation time. The irradiation for 40 and 60 min produces inhibition close to 100%.

The influence of the laser pulse energy (100, 200, 350 and 400 μJ) was investigated in antimicrobial effect is shown in the Fig. 5c. The results show that the highest pulse energy irradiation

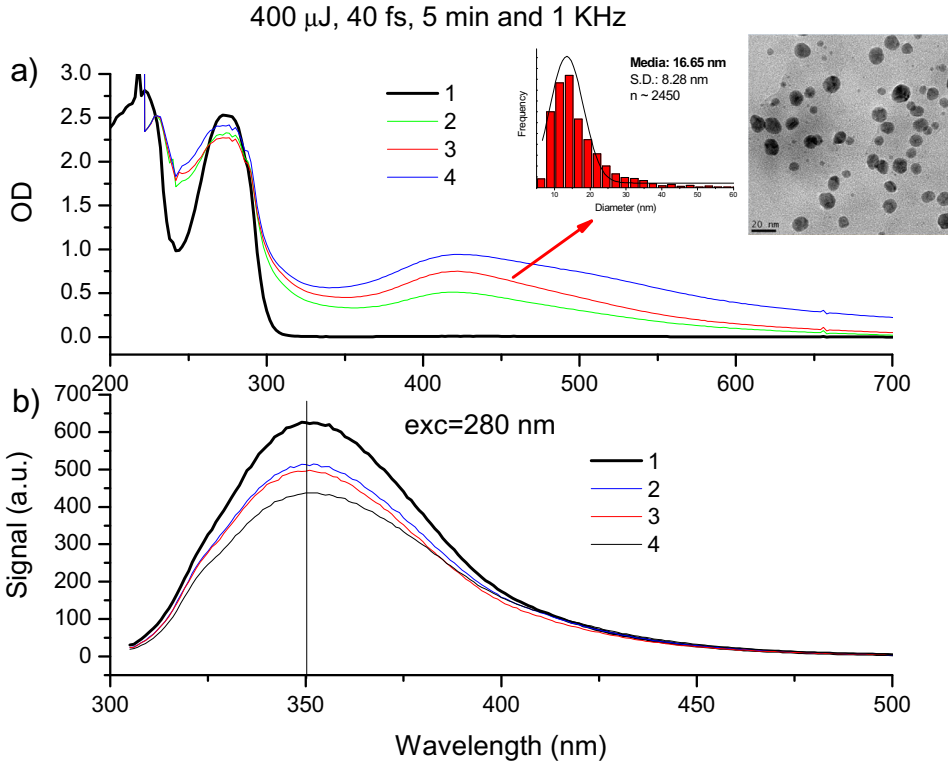

Fig. 1. (a) Optical absorption spectra of samples 1, 2, 3, and 4 after femtosecond laser irradiation for 5 min and solution 3 before irradiation. The size distribution and TEM image (sample 3). (b) Tryptophan fluorescence obtained exciting samples at 280 nm.

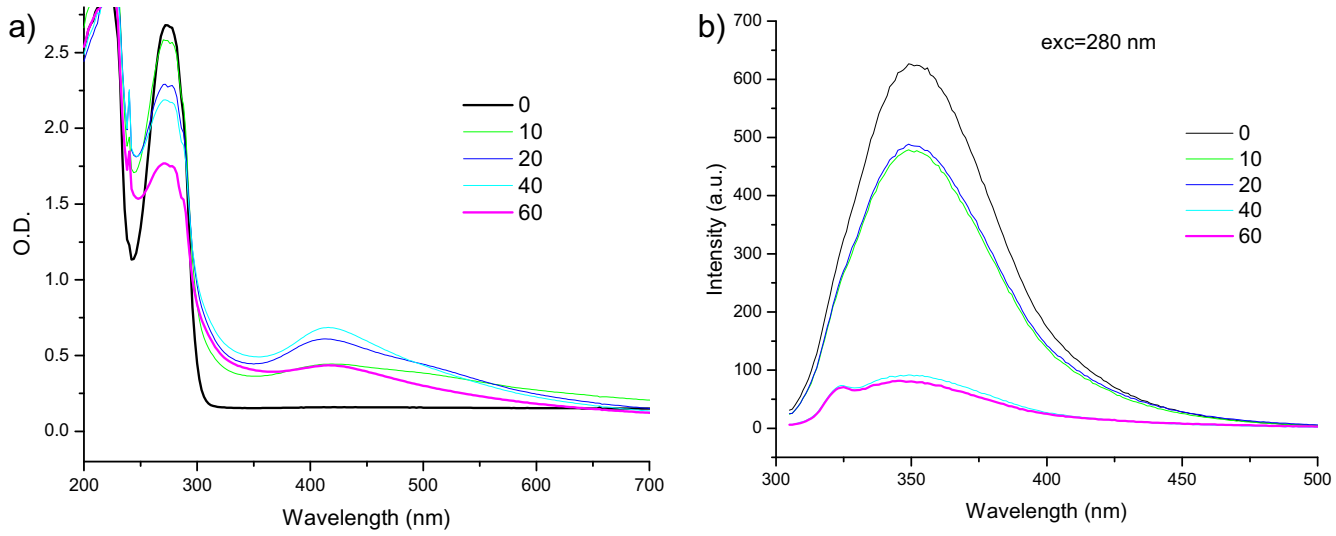

Fig. 2. (a) Absorption spectra of TrpAgNPs (sample 3) not irradiated (G0) and irradiated by 300 μJ ultrashort pulses for 5, 10, 20, 40 and 60 min. (b) Tryptophan fluorescence spectra obtaining exciting samples ~280 nm and the respective absorption spectra.

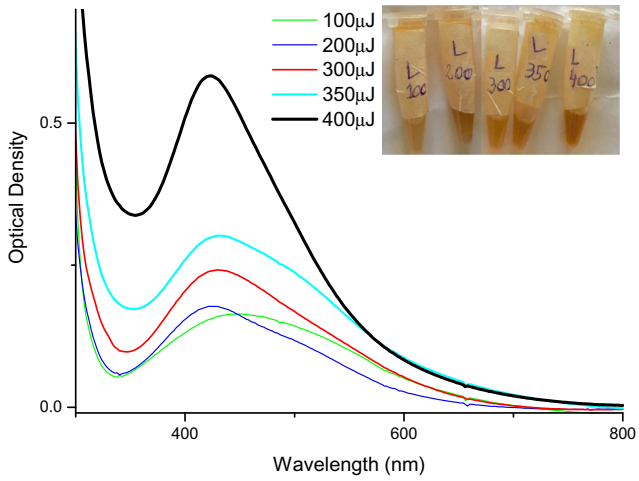

Fig. 3. Absorption spectra and samples photos showing the influence of laser energy 100, 200, 300, 350 and 400 μJ.

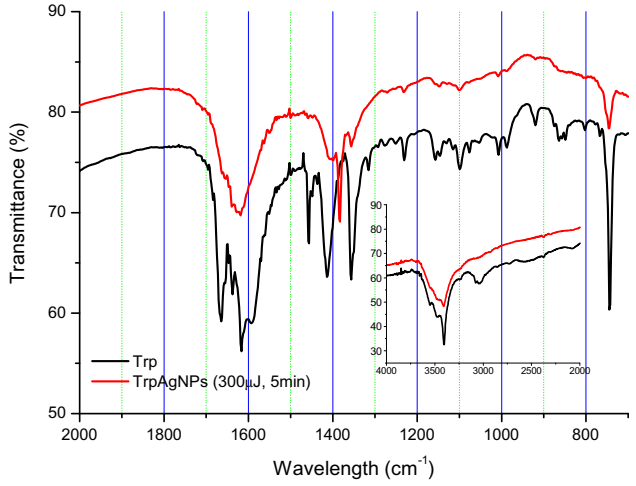

Fig. 4. FTIR spectra of tryptophan and TrpAgNPs before and after laser irradiation.

(400 μJ) is the best condition for bacteria inhibition (almost 100%). Lower energies, and consequently lower TrpAgNPs final concentrations, induces low *E. coli* growth inhibition.

4. Discussion

The position and shape of the SPR absorption of silver nanoparticles are strongly dependent on the particle size, and surface-adsorbed species [12,23,24]. According to Mie's theory, small spherical nanoparticles should exhibit a single SPR band, whereas anisotropic particles should originate two or three bands, depending on their shape [25,26]. The absorption spectra of larger NPs can exhibit broader or additional bands in the UV–Vis range due to the excitation of plasmon resonances or quadrupole and higher multipole plasmon excitations [27]. In this study, different irradiation times and pulse energies were used to produce TrpAgNPs by focusing ultrashort laser pulses in tryptophan and silver nitrate water solutions. We observed the dependence of the SPR spectra of TrpAgNPs, in the range of 200–700 nm, on different concentrations and laser irradiation parameters. The absorption spectra (Fig. 1a) of the TrpAgNPs (40 fs, 400 μJ, 1 kHz, 5 min) shows a SPR absorption band with a maximum around 422 nm. The UV–Vis spectra (Fig. 1a) of solutions 2 and 3 show only one symmetric absorption peak. Monodisperse solutions have a symmetric SPR peak shape, with a small FWHM value. Solution 4 presents an asymmetric SPR band that seems to consist of two or more absorption peaks, and is a polydisperse solution.

In the process of TrpAgNPs formation, a fraction of the tryptophan molecules in the solution are excited by rapidly absorbing photons, and a radical tryptophan cation is formed by charge separation;

$$Trp \xrightarrow{h\upsilon} Trp^{*} \rightarrow Trp^{+} + e^{-} \quad (1)$$

After the reduction, silver clusters are formed with the subsequent nucleation and growth of the nanoparticles. Thus, laser is a catalyst for the formation of the TrpAgNPs.

$$xAg^{+} + nxe^{-} + Trp \rightarrow Ag_{n}^{0}(clusters) \quad (2)$$

Tryptophan also acts as capping and stabilizing agent. Results obtained by FTIR, Fig. 4, indicate that both carboxylate and amino groups of L-Tryptophan are possible terminal groups to attach onto the surface of silver nanoparticles [28].

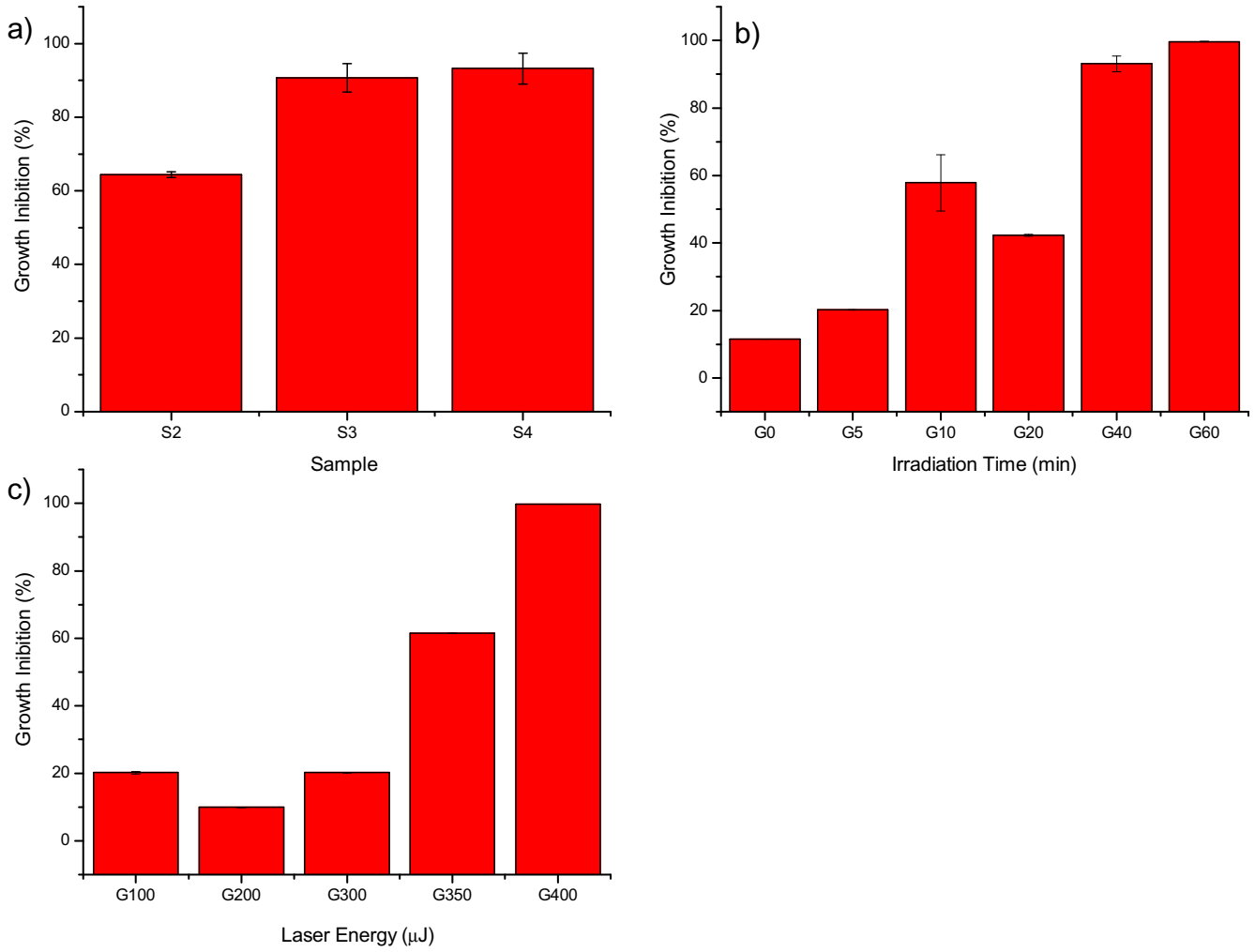

Fig. 5. (a) *E. coli* growth inhibition obtained: (a) with incubation of samples with different $AgNO_3$ concentrations (2, 3 and 4) by 24 h, (b) with incubation with sample 3 irradiated with different time durations: 0, 5, 10, 20 40 and 60 min and (c) sample 3 irradiated with different laser energies: 100, 200, 300, 350 and 400 μJ.

The ultrashort laser pulses induce fragmentation and aggregation processes simultaneously [26,29]. Femtosecond pulses promote tunneling ionization [30] in the nanoparticles, which evolves to avalanche ionization and accumulation of a positive net charge. As a consequence, depending on the laser energy or irradiation duration there is a Coulomb explosion of the particle [19], releasing silver atoms, ions and clusters [19].

Fig. 2a shows the UV–visible absorption spectra of the silver colloid solutions submitted to different irradiation times (40 fs, 300 μJ, 1 kHz, 10, 20, 40 and 60 min). These results indicate that the synthesized TrpAgNPs were initially large, and became smaller under increasing irradiation time.

In previous study it was observed that Tryptophan does not require illumination or heating for producing silver nanoparticles, and the solution color changes immediately after the mixing of reagents if sodium hydroxide is added to the solution (pH = 10) [18]. In this case, sodium hydroxide raises the pH, releases H^+ and allows the reduction of silver ions (Ag^+) to metallic silver (Ag^0). The laser illumination has a similar role as sodium hydroxide in the nanoparticles synthesis and laser parameter control can control the H^+ liberation.

Some of the formed silver particles are re-irradiated by the subsequent laser pulses and fragmented into smaller particles. So, longer irradiation times form smaller NPs monodispersed (Fig. 2a). Irradiation for 10, 20 and 40 min evidencing that the longer irradiation times create more nanoparticles with smaller size dispersion (narrower bands). The increase in the irradiation time to 60 min results in a decrease of the SPR band intensity, probably due to a simultaneous increase in the tryptophan photolysis process. This is evidenced by the decrease in the tryptophan absorption band around 275 nm for irradiation times longer than 20 min, and by the reduction on the tryptophan emission band when the irradiation time increases, shown in Fig. 2b. These effects consistently indicate a reduction on the tryptophan density, which is attributed to its photolysis and the formation of photoproducts as kynurenine and formic acid [31,32]. The oxidation of tryptophan and formation of Kynurenine was described before [17]. Results shown in the Fig. 4 indicate a decrease in the bands of pyrrole suggesting a beginning of conversion of tryptophan to kynurenine in the solutions irradiated by laser for 5 min and 300 μJ. The tryptophan photolysis, destabilize the particles that may form aggregates.

4.1. E. Coli growth inhibition assay

Small and symmetrical NPs exhibiting small size dispersions (narrow SPR bands) have better inhibition against *E. coli* growth compared to the asymmetrical nanoparticles with wider SPR bands and corroborates previously reported findings. Mlalila et al. [33] as reveled by Fig. 5a. Fig. 5b shows that as the irradiation duration increases, the SPR absorption band become sharper, indicating a

decrease in the nanoparticles size dispersion and increase in the bactericidal effect against *E. coli*. The solutions irradiated for 40 and 60 min present a strong bactericidal effect. These solutions promoted 90% growth inhibition after incubation for 24 h. However, the SPR peak decreases for the longest irradiation time (60 min), indicating that TrpAgNPs begin to decay. This fact suggests that another process must be inhibiting the *E. coli* growth, since its inhibitory effects are like those of 40 min solution, which has higher nanoparticles concentration. In Fig. 5c, a decrease in the tryptophan emission band is observed, indicating a strong photolysis process acting upon this molecule. In this situation, the prolonged irradiation time consumes almost all the tryptophan in the solution, increasing the concentration of formic acid and kynurenine (the solution presents a typical formic acid smell), and nearly eliminating the tryptophan available to stabilize the nanoparticles. The tryptophan photoproducts that remain in the solution presents strong lethal effect on *E. coli* [34] and must be the responsible of the *E. coli* apoptosis in sample irradiated by 60 min.

5. Conclusions

This work reports on the synthesis of silver nanoparticles, by means of the femtosecond laser photoreduction of tryptophan water solution and its antimicrobial properties. The use of tryptophan and substitution of solvents by water, and reducing agents by light makes this procedure important from the green chemistry viewpoint. The nanoparticles were characterized by using optical absorption spectroscopy and electron microscopy. The results demonstrated that the nanoparticles concentration plays an important role in *E. coli* bactericidal efficacy. The increase in the laser energy caused an increase in bactericidal effect. The solutions irradiated for longer time durations, 40 and 60 min, present a strong bactericidal effect. However, for solution irradiated for 60 min, the bactericidal activity was attributed to the presence of tryptophan photoproducts.

Acknowledgments

The authors acknowledge the National Council for Scientific and Technological Development (CNPq) and the São Paulo State Research Support Foundation (FAPESP) grant 2014/06960-9 for financial support, and a PAP scholarship (Secretariat of Health) given to Daniella dos Santos Courrol.

Conflict of interest

The authors declare that they have no conflict of interest.

References

[1] M.J. Sweet, A. Chesser, I. Singleton, Review: metal-based nanoparticles size, function, and areas for advancement in applied microbiology, Adv. Appl. Microbiol. 80 (80) (2012) 113–142.
[2] J.M. Schierholz, L.J. Lucas, A. Rump, G. Pulverer, Efficacy of silver-coated medical devices, J. Hosp. Infect. 40 (1998) 257–262.
[3] L. Rizzello, R. Cingolani, P.P. Pompa, Nanotechnology tools for antibacterial materials, Nanomedicine 8 (2013) 807–821.
[4] S. Silver, Bacterial resistances to toxic metal ions – a review, Gene 179 (1996) 9–19.
[5] M. Rai, A. Yadav, A. Gade, Silver nanoparticles as a new generation of antimicrobials, Biotechnol. Adv. 27 (2009) 76–83.
[6] A. Panacek, L. Kvitek, R. Prucek, M. Kolar, R. Vecerova, N. Pizurova, V.K. Sharma, T.J. Nevecna, R. Zboril, Silver colloid nanoparticles: synthesis, characterization, and their antibacterial activity, J. Phys. Chem. B 110 (2006) 16248–16253.
[7] L.C. Courrol, F.R.d.O. Silva, L. Gomes, A simple method to synthesize silver nanoparticles by photo-reduction, Colloids Surfaces A – Phys. Eng. Aspects 305 (2007) 54–57.
[8] R.A. de Matos, T.d.S. Cordeiro, R.E. Samad, L.B. Sicchieri, N.D. Vieira Junior, L.C. Courrol, Synthesis of silver nanoparticles using agar-agar water solution and femtosecond pulse laser irradiation, Colloids Surfaces A – Physicochem. Eng. Aspects 423 (2013) 58–62.
[9] J. Lee, M. Lee, Laser-induced conversion of Au powders to highly stable nanoparticles with a narrow size distribution, J. Phys. Chem. C 120 (2016) 13256–13262.
[10] A. Ivask, A. ElBadawy, C. Kaweeteerawat, D. Boren, H. Fischer, Z.X. Ji, C.H. Chang, R. Liu, T. Tolaymat, D. Telesca, J.I. Zink, Y. Cohen, P.A. Holden, H.A. Godwin, Toxicity mechanisms in escherichia coli vary for silver nanoparticles and differ from ionic silver, ACS Nano 8 (2014) 374–386.
[11] P. Korshed, L. Li, Z. Liu, T. Wang, The molecular mechanisms of the antibacterial effect of picosecond laser generated silver nanoparticles and their toxicity to human cells, Plos One 11 (2016).
[12] M.A. Raza, Z. Kanwal, A. Rauf, A.N. Sabri, S. Riaz, S. Naseem, Size- and shape-dependent antibacterial studies of silver nanoparticles synthesized by wet chemical routes, Nanomaterials 6 (2016).
[13] A. Dror-Ehre, H. Mamane, T. Belenkova, G. Markovich, A. Adin, Silver nanoparticle-E. coli colloidal interaction in water and effect on E-coli survival, J. Colloid Interface Sci. 339 (2009) 521–526.
[14] R.J. Tomita, R.A. de Matos, M.A. Vallim, L.C. Courrol, A simple and effective method to synthesize fluorescent nanoparticles using tryptophan and light and their lethal effect against bacteria, J. Photochem. Photobiol. B-Biol. 140 (2014) 157–162.
[15] S.K. Srivastava, T. Hasegawa, R. Yamada, C. Ogino, M. Mizuhata, A. Kondo, Green synthesis of Au, Pd and Au@ Pd core-shell nanoparticles via a tryptophan induced supramolecular interface, RSC Adv. 3 (2013) 18367–18372.
[16] I.O. Shmarakov, I.P. Mukha, V.V. Karavan, O.Y. Chunikhin, M.M. Marchenko, N. P. Smirnova, A.M. Eremenko, Tryptophan-assisted synthesis reduces bimetallic gold/ silver nanoparticle cytotoxicity and improves biological activity, Nanobiomedicine 1 (2014).
[17] I. Mukha, N. Vityuk, O. Severynovska, A. Eremenko, N. Smirnova, The pH-dependent stucture and properties of Au and Ag nanoparticles produced by tryptophan reduction, Nanoscale Res. Lett. 11 (2016).
[18] R.A. de Matos, L.C. Courrol, Biocompatible silver nanoparticles prepared with amino acids and a green method, Amino Acids 49 (2017) 379–388.
[19] D. Werner, A. Furube, T. Okamoto, S. Hashimoto, Femtosecond laser-induced size reduction of aqueous gold nanoparticles: situ and pump-probe spectroscopy investigations revealing coulomb explosion, J. Phys. Chem. C 115 (2011) 8503–8512.
[20] G.K. Wang, Y.F. Lu, H.M. Hou, Y.F. Liu, Probing the binding behavior and kinetics of silver nanoparticles with bovine serum albumin, RSC Adv. 7 (2017) 9393–9401.
[21] P. Joshi, V. Shewale, R. Pandey, V. Shanker, S. Hussain, S.P. Karna, Tryptophan-gold nanoparticle interaction: a first- principles quantum mechanical study, J. Phys. Chem. C 115 (2011) 22818–22826.
[22] R. Dojcilovic, J.D. Pajovic, D.K. Bozanic, V.V. Vodnik, S. Dimitrijevic-Brankovic, A.R. Milosavljevic, S. Kascakova, M. Refregiers, V. Djokovic, A fluorescent nanoprobe for single bacterium tracking: functionalization of silver nanoparticles with tryptophan to probe the nanoparticle accumulation with single cell resolution, Analyst 141 (2016) 1988–1996.
[23] S.L. Zhu, W. Zhou, Optical properties and immunoassay applications of noble metal nanoparticles, J. Nanomater. 12 (2010).
[24] P.K. Jain, X. Huang, I.H. El-Sayed, M.A. El-Sayad, Review of some interesting surface plasmon resonance-enhanced properties of noble metal nanoparticles and their applications to biosystems, Plasmonics 2 (2007) 107–118.
[25] K. Kolwas, A. Derkachova, M. Shopa, Size characteristics of surface plasmons and their manifestation in scattering properties of metal particles, J. Quant. Spectrosc. Radiat. Transfer 110 (2009) 1490–1501.
[26] P.V. Kamat, Photophysical, photochemical and photocatalytic aspects of metal nanoparticles, J. Phys. Chem. B 106 (2002) 7729–7744.
[27] P.V. Kamat, M. Flumiani, G.V. Hartland, Picosecond dynamics of silver nanoclusters. Photoejection of electrons and fragmentation, J. Phys. Chem. B 102 (1998) 3123–3128.
[28] C.H. Chuang, Y.T. Chen, Raman scattering of L-tryptophan enhanced by surface plasmon of silver nanoparticles: vibrational assignment and structural determination, J. Raman Spectrosc. 40 (2009) 150–156.
[29] K. Maximova, A. Aristov, M. Sentis, A.V. Kabashin, Size-controllable synthesis of bare gold nanoparticles by femtosecond laser fragmentation in water, Nanotechnology 26 (2015).
[30] A. Royon, Y. Petit, G. Papon, M. Richardson, L. Canioni, Femtosecond laser induced photochemistry in materials tailored with photosensitive agents Invited, Opt. Mater. Express 1 (2011) 866–882.
[31] R.F. Borkman, L.B. Hibbard, J. Dillon, The photolysis of tryptophan with 337.1 nm laser-radiation, Photochem. Photobiol. 43 (1986) 13–19.
[32] Y. Fukunaga, Y. Katsuragi, T. Izumi, F. Sakiyama, Fluorescence characteristics of kynurenine and N′-formylkynurenine – their use as reporters of the environment of tryptophan-62 in hen egg-white lysozyme, J. Biochem. 92 (1982) 129–141.
[33] N.G. Mlalila, H.S. Swai, A. Hilonga, D.M. Kadam, Antimicrobial dependence of silver nanoparticles on surface plasmon resonance bands against Escherichia coli, Nanotechnol. Sci. Appl. 10 (2017) 1–9.
[34] K.F. Over, N. Hettiarachchy, M.G. Johnson, B. Davis, Effect of Organic Acids and Plant Extracts on Escherichia coli O157:H7, listeria monocytogenes, and salmonella typhimurium in broth culture model and chicken meat systems, J. Food Sci. 74 (2009) M515–M521.